Ruben Enrico Visser

BIO-BASED FLUORESCENT CARBON DOTS FOR NANOTHERMOMETRY

MASTER'S DEGREE THESIS

Supervised by Dr Maria Cinta Pujol and Dr Joan Josep Carvajal

MASTER'S DEGREE IN NANOSCIENCE, MATERIALS AND PROCESSES

UNIVERSITAT ROVIRA i VIRGILI

Tarragona

2024

BIO-BASED FLUORESCENT CARBON DOTS FOR NANOTHERMOMETRY

Ruben Enrico Visser
Master's Degree in Nanoscience Materials and Processes (2023-2024)
Supervisors: Dr Maria Cinta Pujol and Dr Joan Josep Carvajal
Department of Physical and Inorganic Chemistry. Universitat Rovira i Virgili,
Campus Sescelades, Marcel·lí Domingo 1, Tarragona 43007, Spain.

Abstract

Carbon dots (CDs) have received significant scientific attention for their fluorescence, low toxicity, and biocompatibility, making them ideal for applications in (bio-)sensing, bioimaging, and nanothermometry. However, challenges persist in synthesizing CDs from sustainable, bio-based precursors and tuning their fluorescence to the red region for relevant applications. This study addresses both issues by synthesizing CDs from xylose extracted from almond shells, a bio-waste material, and doping them with phenylenediamine to achieve red-shifted fluorescence. The synthesized CDs were characterized using TEM and photoluminescence spectroscopy, demonstrating successful particle formation and tuneable fluorescence. Temperature-dependent fluorescence measurements indicated that the doped CDs could serve as effective temperature sensors, showing sensitivity within the biological temperature range. Despite some limitations, this holistic investigation highlights the potential of bio-based, red-emissive CDs for sustainable nanothermometry applications.

1 INTRODUCTION

Carbon Dots (CDs) have received growing scientific attention since their discovery in 2004, reaching more than 10,000 publications in 2022.[1] Their fluorescence, low toxicity, and biocompatible properties allow for applications in (bio)sensing, (bio)imaging, photocatalysis and optoelectronics.[1-3] Additionally, using CDs for temperature sensing and imaging on the nanoscale has recently been investigated due to their temperature-dependent fluorescence and nanometric size.[4,5] This nano-scale temperature sensing, also referred to as nanothermometry, is an important tool for advancing our understanding of temperature-sensitive processes in biological and chemical systems.

Moreover, alternative fluorescent chemicals and nanomaterials that can be used for nanothermometry are also being investigated like dyes, inorganic nanoparticles, lanthanide-doped nanoparticles, and semiconductor quantum dots.[5] However, these alternatives pose challenges and might not be desirable due to the toxicity of their inorganic precursors, difficult synthesis methods, or fossil-based production processes. Moreover, these alternatives often use source materials that the EU categorizes as critical raw materials due to their supply risks.[6] Bio-based fluorescent CDs, synthesized from renewable or recycled bio- waste, could form a more sustainable and desirable fluorescent material for nanothermometry as well as the other applications mentioned above.

So, as indicated in the articles referenced above, CDs have been well studied and show promise for novel applications. However, there are still challenges that need to be addressed before effective integration into relevant applications. Two of these challenges will be discussed here. One problem is that CD research has mainly focused on synthesis methods where highly purified commercially available precursors were selected. These precursors are often produced from fossil sources or through elaborate chemical processes.[1, 7-9] With the current global need for reducing our dependence on fossil resources, alternatives should be investigated. Another aspect of this first problem is that some studies have already explored synthesis routes that mimic the production of bio-based carbon dots using biomolecules potentially extractable from biomass.[10-13] However, these studies used commercially available and highly purified precursors. This means that they do not properly account for the differences and difficulties that can arise when you are not using highly purified

precursors but are instead using biomolecules directly extracted from bio-waste.

The second challenge that is of interest in CD synthesis and engineering is tuning the fluorescence excitation and emission to the red region for optimal use in biological systems. This red shift is also critical for effective use of CDs in nanothermometry. Longer wavelength red light shows low absorption and deeper penetration in biological tissues, reduced scattering, reduced photodamage, and weak background biological fluorescence.[7,9] So, tuning CD fluorescence to longer wavelength excitation and emission is of great interest, and research efforts have demonstrated methods to achieve this.

Previous studies have identified multiple CD properties that can be tuned to achieve longer wavelength fluorescence. In CDs that contain a graphitic core, a larger core size results in a longer wavelength of the dominant emission peak.[3, 14] This is attributed to the quantum confinement effect, an effect that reduces the bandgap when particles become smaller, which is also present in quantum dots. So, tuning the size could be an effective method to achieve longer wavelength emission. Additionally, functional chemical groups on the surface of the CDs are linked to a dramatic shift in the fluorescence properties by influencing the electronic structure, especially when directly bonded and conjugated with the graphitic core. This effect could be used to shift the fluorescence towards red emission. However, this phenomenon is still being investigated and up for debate.[3, 15]

A more clearly understood strategy for tuning the emission wavelength of CDs is the controlled introduction of heteroatoms into the CD lattice by means of doping.[16, 17] The introduction of heteroatoms changes the electronic structure of these structures and thus the interaction between carbon dots and light. Nitrogen doping, due to the similar atomic size and its five valence electrons, has been highlighted as an effective approach to improve fluorescence, and the used ratio of nitrogen-dopant can shift the fluorescent wavelength.[17, 18] More specifically, the molecule phenylenediamine has been effectively used for tuning carbon dots for red fluorescence, especially carbon dots containing the *ortho* isomer have been reported to show emission at longer wavelengths.[19]

The two challenges of using bio-waste feedstocks and engineering for red-fluorescence have been overcome by some studies referred to above, however to the best of our knowledge there are no studies that attempt to tackle both challenges and report on bio-based CDs with longer wavelength emission in a holistic investigation.[10, 12, 13] The holistic investigation described in this thesis will attempt to include both aspects. In this report, bio-based CDs synthesized from xylose extracted from biomass and doped with the organic compound phenylenediamine will be investigated. This will be executed with the intention to study if these CDs can effectively be utilized for nanothermometry, considering the specific properties that are needed for this application. A hydrothermal synthesis method will be employed to fabricate doped-CDs and an investigation into the nanostructure and optical properties will allow for conclusions to be drawn.

2 EXPERIMENTAL

When synthesising and investigating CDs a couple of important methodological aspects should be considered. The characterization techniques, with the accompanying result-interpretation challenges, will be discussed in the results and discussion sections. However, the general experimental method, the CD purification, and the selected precursors used in this study will be discussed here

2.1 MATERIAL & METHOD INTRODUCTION

Regarding the synthesis method that is suitable for bio-based CD synthesis, this report, like other bio-based CD studies, will focus on a bottom-up hydrothermal synthesis method. Hydrothermal synthesis is a relatively facile, ecofriendly, and affordable method to produce doped-CDs in which the precursors and water are heated to moderate temperatures in a sealed container.[17] This method is advantageous due to the one-step nature and the ability to directly use biomolecules after extraction with minimal further processing steps.

The bio-based precursors that can be used are biomolecules extracted from lignocellulosic biomass.[1] Additionally, depending on the available biomass source-material, the precursors and their relative abundance in the biomass will change. When selecting a suitable biomass source, one should ideally work with something that is readily available as waste in their local area. This report will focus on using xylose extracted from almond shells originating from local agricultural waste material here in Spain. Not only is Spain one of the largest producers of almonds worldwide, but almonds are also suitable due to their high xylan/xylose content.[20]

Moreover, xylose is appropriate to use due to previous proven synthesis routes for xylose-CDs.[10, 12, 13] The xylose used in this investigation was extracted in a routine way from almond shells. Details on the xylose extraction procedure can be found in the supporting information (**S.I. 6.3**). In addition to extracted xylose from almond shells, the precursor in this study due to its previously mentioned red-shifting property when used as a dopant.[19]

Name	Xylose (%wt)	*o*-PD (%wt.)	Synthesis time (hour)	Synthesis temp. (°C)	Approximate pH before synthesis	Approximate pH after synthesis
CD-6h	100	N.A.	6	200	3	2
CD-6h-pH7	100	N.A.	6	200	7	3
CD-6h-10%	90	10	6	200	4	2
CD-6h-25%	75	25	6	200	5	4
CD-6h-50%	50	50	6	200	5	5
CD-12h	100	N.A.	12	180	3	2
CD-12h-pH7	100	N.A.	12	180	7	3
CD-12h-10%	90	10	12	180	4	2
CD-12h-25%	75	25	12	180	5	4
CD-12h-50%	50	50	12	180	5	5

Table 1: Names, synthesis parameters and pH of the discussed samples.

2.2 SYNTHESIS & PURIFICATION

The synthesis of the CQDs derived from almond shells was performed by a conventional hydrothermal method. The reaction was carried out by adding 500 mg (±2mg) of the precursor(s) to a beaker with 20 ml of deionized water measured with a chemical balance and a volumetric pipette. The precursor(s) were stirred with a spatula and the solution was sonicated for 15 minutes to fully dissolve the solids. For the reactions that required the pH to be controlled, CD-6h-pH7 and CD-12h-pH7 (*Table 1*), an amount of ammonia was added to the solution. The ammonia was stirred in with a spatula to homogenize. The hydrothermal reactions were started by transferring the solution to a Teflon-lined stainless-steel autoclave (*Figure 1*) placed in a muffle oven. After the heating stage, the autoclave was let to cool to room temperature before transferring the suspension to a beaker. The beaker was placed in an ultrasonic bath for 15 minutes to redistribute any agglomerates. The suspension was then filtered through a 0.2 µm syringe filter. The filtrate was collected and transferred to a 1000 Da dialysis membrane in 1L of deionized water, as can be seen in *Figure 1*. The 1L beaker containing the dialysis membrane was gently stirred for at least 24 hours at room temperature before changing the dialyzate for fresh deionized water. A sample was collected of the discarded dialyzate before stirring the membrane for at least another 24 hours. The resulting liquid inside the dialysis membrane was collected in an opaque vial and stored in a fridge at approximately 5 °C for further characterization and use. The names and synthesis parameters of the dialyzed samples can be found in *Table 1.*

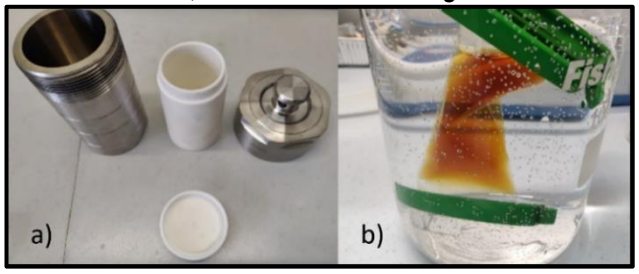

Figure 1: a): Teflon-lined stainless-steel autoclave. b): Example of dialysis setup.

2.3 CHARACTERIZATION

For Transmission Electron Microscopy (TEM) imaging, two drops of the dialyzed samples were dopped on a High-Resolution TEM (HR-TEM) compatible copper and carbon grid. The grids were let to dry overnight before being transferred to the *JEOL* HR-TEM equipment (*JEM-F200*). Using software (ImageJ & GATAN Digital Micrograph®) the particle diameters were measured to determine the size distributions and determining the interplanar distance was done using Fast Fourier Transfer image analysis.

For photoluminescence measurements, a small amount of liquid sample was transferred to a quartz cuvette and placed in the *Zolix* fluorescence spectrometer (*OmniFluo900*). Dialyzed products were measured as well as some precursor solutions before any hydrothermal reaction was performed. Emission spectra were recorded for excitation wavelengths from 305 nm to 500 nm with 25 nm intervals. An excitation spectrum was recorded for the unique wavelength that resulted in the most intense fluorescent peak in the emission spectrum of each sample. Bandwidths of 3 nm were used for excitation and detection, and 1 nm steps for the recorded spectra.

Additional photoluminescence measurements were taken using the *Horiba* fluorescence spectrometer (*Fluorolog*) equipped with a Peltier heating module sample holder. Again, the liquid samples were transferred to a quartz cuvette and placed in the Peltier heater. First, two emission spectra were recorder at room temperature (25 °C) at 305 nm and 372 nm excitation. These wavelengths were selected because at room temperature relatively intense emission peaks were found at these excitation wavelengths for the doped samples. Subsequently, the temperature of the heating module was increased with steps of 10 °C until 75 °C (covering the biological temperature range) and the two spectra were

recorded at each temperature. For a full list of the used chemicals and equipment see **S.I. 6.1 & 6.2**

3 RESULTS & DISCUSSION

3.1 EXPERIMENTAL PROCESS

Throughout the synthesis and purification process the color and opacity of the liquid samples changed. Each time starting out as an opaque light orange solution and changing to a black suspension after the synthesis process. Notably, the doped samples had a slight red/brown color after synthesis which become more apparent with higher amounts of doping, see *Figure 1* b), and *Figure 2* d). For the undoped samples, the solutions became yellow and clear after filtration, and colorless and clear after dialysis. This was different for the doped samples. The doped samples maintained some of the red/brown color after filtration, and after dialysis they were clear with a slight yellow color. The black suspension that was present in all samples is a clear indication that the temperature and pressure during the hydrothermal reactions were sufficient for the carbonization process to occur, as can be seen in image a in *Figure 2*. Furthermore, the observed differences between the samples clearly indicate that the optical properties of these samples have changed by the addition of the dopant. This becomes apparent in *Figure 2* image b) and d), where a clear difference between the color of an undoped (b) and 25% doped (d) sample at the stage after filtration and before completing dialysis can be seen. An additional example can be seen in *Figure 1* image b) showing a sample doped by 10%.

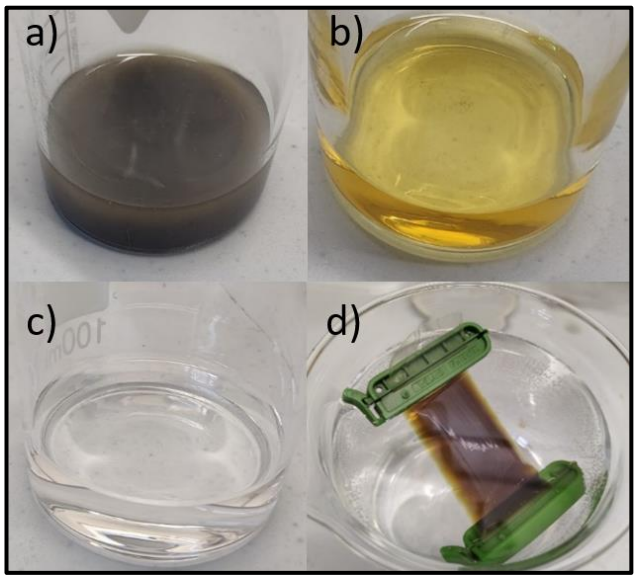

Figure 2: a): CD-6h before filtration. b): CD-6h after filtration. c): CD-6h after dialysis. d): Start of dialysis of a doped sample.

Another aspect that had a considerable effect during the synthesis process is the acidity of the precursor solution. It has been reported that the reactions that occur in the formation of carbon dots are catalyzed by acid.[21] This catalytic effect also played a role in the experiments in this report. Due to the use of sulfuric acid in the almond shell extraction process, some amount of acid was present in the extracted xylose solid. As a result, the amount of extracted xylose that was dissolved determined the pH of the solution, as can be seen in *Table 1*. The exception here are the two samples that had a pH of 7 before synthesizing. These two samples had their pH manually increased by adding ammonia until it reached a value of 7. This resulted in measurably different optical and physical properties in the resulting material. Namely a shift to shorter wavelength fluorescence and noticeably less particles being detected, as can be seen in *Figure 5*. A notable effect of the different pH starting values in the synthesis and purification process was observed during the filtration. A clear trend was observed that made the pressure required to push the liquid sample through the syringe filter much higher when the starting pH was higher. Less pressure was required for the samples that had a lower starting pH. This might indicate that particle sizes are dependent on the acidity of the solution. This effect has been studied before, which revealed that acids promote carbonization and dehydration, increasing particle sizes and effectively catalyzing the CD-forming reactions.[21]

3.2 ELECTRON MICROSCOPY

The HR-TEM imaging of the doped and undoped samples shows particles with average sizes below 30 nm, as can be seen in *Figure 3*. The undoped samples CD-6h and CD-12h have an average size of 3.5 nm and 4.5 nm respectively. The doped samples shown here, CD-6h-10%, CD-12h-25% and CD-12h-50%, have average sizes of 7 nm, 16 nm and 26 nm respectively. Both the doped and undoped samples display a trend where a longer reaction time yields larger particles, this trend can be expected considering the nucleation and subsequent growth have more time to continue. Additionally, a less obvious trend was observed where particle sizes increase with increasing amounts of *o*-phenylenediamine doping. This suggests that the presence of the dopant modifies the surface energy of the growing particles, ultimately increasing their final size.

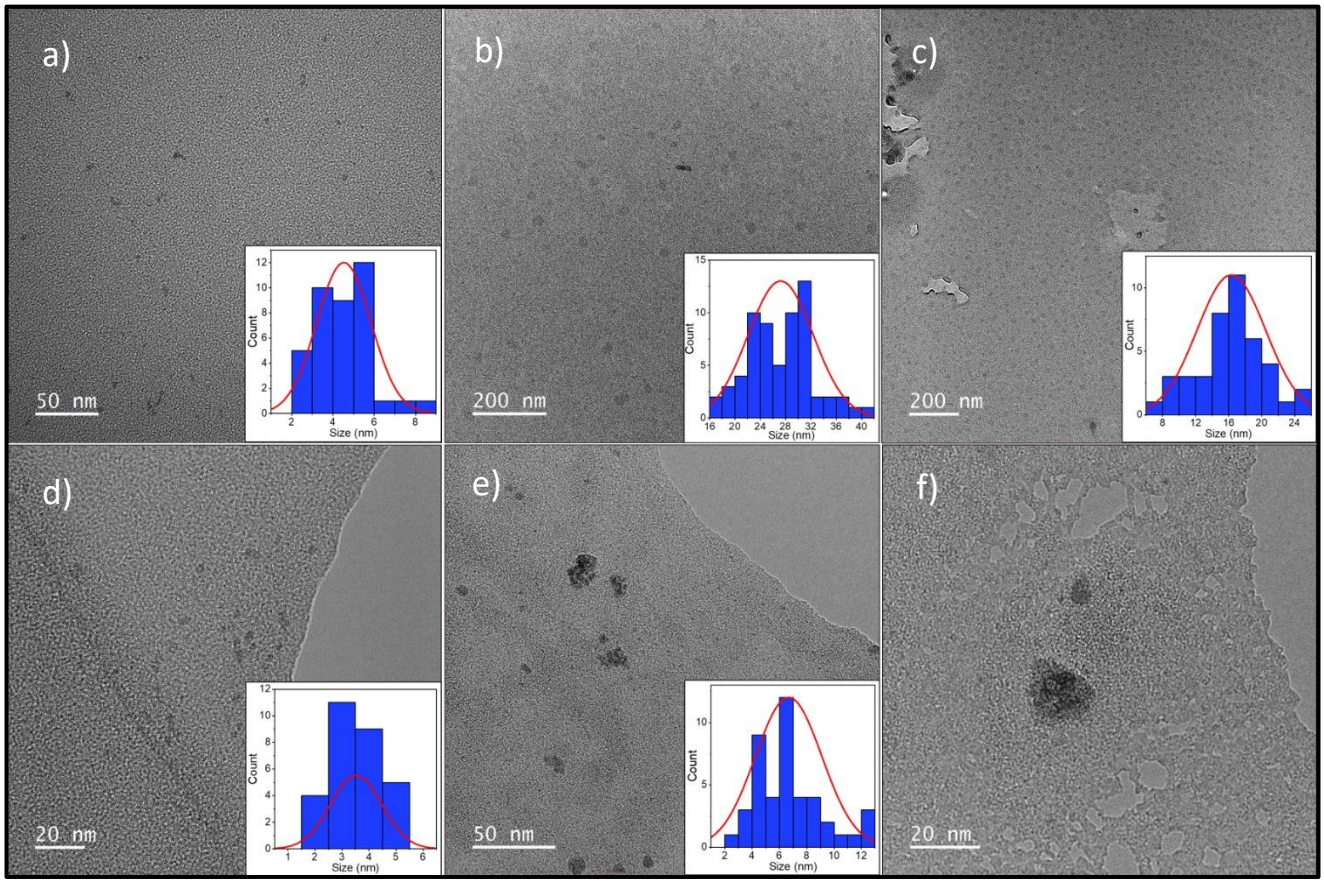

Figure 3: HR-TEM and particle size distribution of a): CD-12h. b): CD-12h-25%. c): CD-12h-50%. d): CD-6h. e & f): CD-6h-10%.

Regarding the morphology, the observed particles have a predominantly circular shape, with some more elongated and irregular shapes present. Particle size analysis further revealed a relatively narrow distribution for the undoped samples compared to the doped samples, suggesting a higher degree of uniformity in the former.

In some HR-TEM images a clear stacking can be seen. This stacking was used to calculate lattice spacing of the particles. Lattice spacing of 0.24(±1) and 0.34 nm have been found. These are values that have previously been found for CDs and can be attributed to the (100) and (002) crystal planes of graphite.[1] Although some samples exhibit this crystallinity, for most of the observed particles there was no clear crystallinity. These variations in size, shape, and crystallinity could be explained by the fact that the precursor in this study, extracted xylose, is not as chemically pure compared to most CD synthesis processes described in literature. However, these variations are not uncommon for CDs, especially when comparing to other reports about lignocellulosic CDs.[1] Still, the electron imaging has confirmed that with the materials and processes

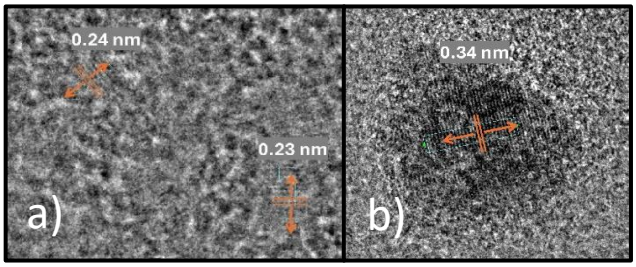

Figure 4: HR-TEM images including the calculated lattice spacing of a): CD-6h and b): CD-6h-10%.

described in this report CDs have been successfully produced.

3.3 PHOTOLUMINESCENCE

The photoluminescence measurements of all the CD samples showed that the samples are fluorescent with emission between 350 and 550 nm. Moreover, all samples show excitation wavelength dependent emission in this range. For the undoped samples, single-band emission was measured with a maximum emission intensity around 475 nm when excited at 375 nm, as can be seen in *Figure 5* a) which displays spectra at room temperature. Image b) in this figure clearly shows a substantial shift in emission to shorter wavelengths as an effect of the starting pH of the synthesis process. The effect of pH was investigated

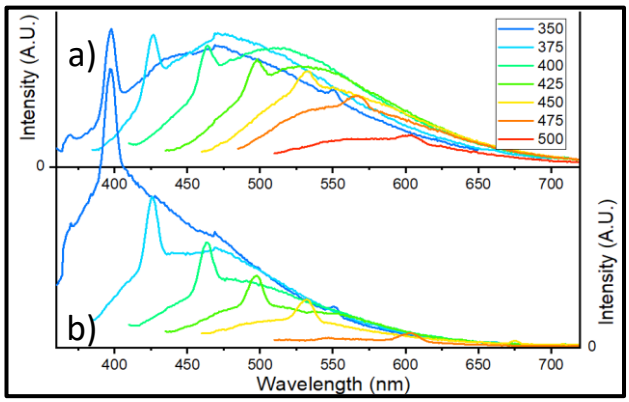

Figure 5: Photoluminescence spectra at room temperature with the different colors representing the excitation wavelength for sample a): CD-6h and b): CD-6h-pH7. The sharp peak present in these samples is produced by water, as can be seen in ***SI. 6.3.1.***

before the doping experiments were conducted. This led to the conclusion that the native acid in the. extracted xylose was desirable due to the undesirable blue-shift that was associated with higher pH values

The following aspect to look at considering the desired emission for thermometric applications is the engineering for longer wavelength emission. A representative emission spectrum of a doped sample can be found in *Figure 6* a) where the excitation dependent emission is visible. The three emission bands are located around 350, 450 and 525 nm with the latter two being of interest with the application in mind. *Figure 6* b), c) & d) show the shifting of the emission band as an effect of increased doping levels at room temperature for two different excitation wavelengths. Here, it can be concluded that doping caused a slight blue-shift at 375 nm excitation. However, increased doping caused red-shift in the emission when exciting at 400 nm. Up to 66 nm shift was detected when considering the emission peaks of CD-6-10% and CD-6-50%. largest shift of 74 nm was measured between the emission peaks of CD-12-10% and CD-12-50%. It is interesting to note that for the samples doped with 10% there is a consistent blue-shift compared to 0% doping, in contrast to the samples doped with 25/50%. So, the luminescent mechanism at play here is not obvious. This trend might be an effect of the increasing sizes that have been measured with increased doping levels.

Finally, it is important to briefly mention the stability of the samples. To test this, a luminescence spectrum was measured of the undoped sample CD-12h after freeze-drying, storing in a conventional fridge for more than a week, and redispersing the solids in

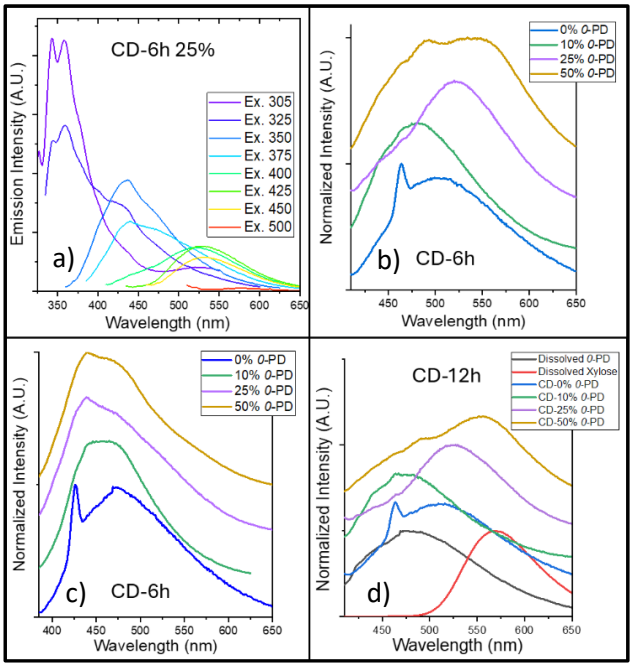

Figure 6: Photoluminescence spectra of different levels of doping. Image a) shows a full emission spectrum of a doped sample representative of the other doped samples. Image b) and d) show the emission bands at 400 nm excitation and c) at 375 nm. Image d) additionally shows the emission of two unreacted solutions of the precursors; extracted xylose (0.5 g in 20 ml), and ortho-phenylenediamine (0.125 g in 20 ml).

water. The spectrum can be found in the supporting information (**6.4.1**) The emission of this sample did not significantly change after this process, indication that the particles are stable, at least when not doped. With this stability, in addition to the discussed optical properties in mind, it can be concluded that the process described here yielded stable CD's that can effectively be engineered by doping with *ortho*-phenylenediamine.

3.4 TEMPERATURE SENSING

As shown in *Figure 7* emission spectra were measured in the range between 25 and 75 °C for investigating the potential of the doped CDs as temperature sensors. In the two samples that were measured the emission intensity decreased as a function of the temperature. This effect can be exploited in multiple ways for application as a temperature sensor, of which two will be discussed here. The first and most straightforward being single-band (SB) luminescence thermometry. To obtain a representative value for the emission intensity, an integral was taken as visualized in *Figure 7*, resulting in the data shown in *Figure 8* a) and b). Using this data, temperatures can be measured by measuring fluorescence intensity of the doped-CDs, although higher precision can potentially be achieved with other approaches.[22] The most promising candidate for this application, CD-6h-50% excited at 375 nm, has the highest measured change in intensity of 24% and additionally shows the most linear decrease, as can be seen in *Figure 8* b). This sample is also the one that will be analyzed for the second approach.

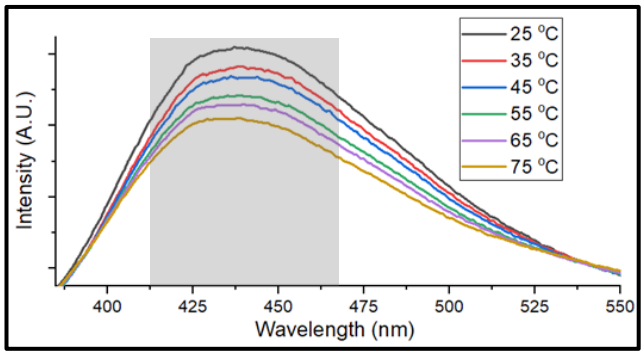

Figure 7: Temperature dependent emission of CD-6h-50% when excited at 375 nm. The gray area shows the range that was used for calculating the emission intensity integrals.

The other method of temperature sensing depends on the ratio of two emission intensities generated by excitation at two different excitation wavelengths.[23] In this case the spectra of sample CD-6h-50% at 305 nm and 375 nm excitation were used. In these two spectra the same wavelength range will be used in a single emission band. This so-called SB ratiometric (SBR) approach is self-referencing and has lower sensitivity to disturbances, in contrast to SB, however it does require additional calculations which have been discussed prior.[22, 23] In the two emission

spectra, an integral was taken with the same limits to obtain intensity values. The ratio between these values was calculated to produce *Figure 8* c). A linear function was fitted in this graph which could then be used to calculate the relative thermal sensitivity, as was also done with the fitted line in image b). This allowed us to compare the two approaches which can be seen in *Figure 8* d). The more sensitive approach presented here is SB luminescence thermometry with a value of -0.62 (%*K^{-1}), this is a (absolute) value in the typical sensitivity range for CDs, although higher sensitivity has been achieved previously.[4]

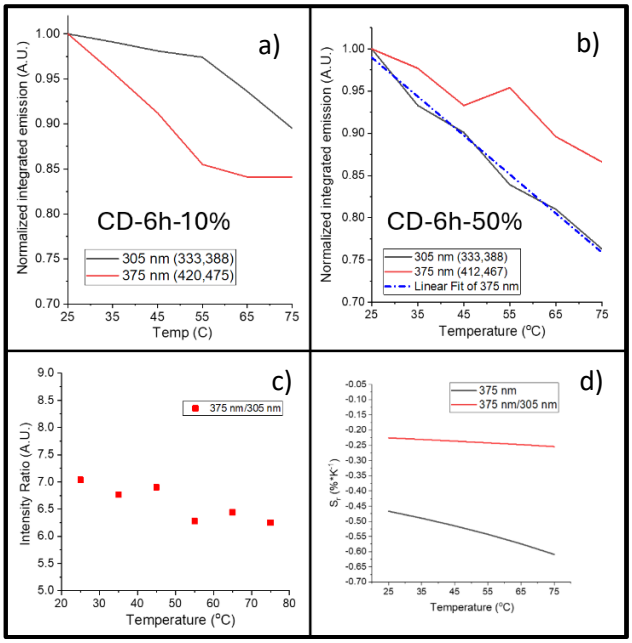

Figure 8: Image a) & b) show the normalized and integrated intensity values over the measured temperature range for excitation at two wavelengths. The values in brackets indicate the limits of the integral which had a range of 55 nm centered around the peak intensity values. Image c) shows the single-band intensity ratio as a function of temperature for sample CD-6h-50% and d) shows the relative thermal sensitivities calculated for the two approaches.

3.5 OPPORTUNITIES AND SHORTCOMINGS

The discussed results in this report have highlighted the potential that bio-based nitrogen doped xylose-CDs have for the use in temperature sensing. However, some methodological aspects of this report should be discussed because a few limitations and shortcomings have been identified. To begin, it is important to point out that the extracted xylose precursor is of unknown purity. Hence no characterization was done to identify the chemical composition. This leads to the possibility that there could be additional biomolecules in the precursor that influence the synthesis and properties that have been discussed. Moreover, for a better understanding of the effect of non-commercially purified precursors a more comprehensive investigation would be required, considering different biomass sources.

Secondly, for a better understanding of the opportunities of engineering CDs for desired

properties, it will be worthwhile to investigate a broader range of doping levels of *ortho*-phenylenediamine, and additionally investigate the effect of the *meta*- and *para*- isomers of the molecule, which have been proven to also influence luminescence properties.[7,11,15,18]

Finally, the luminescent properties discussed in this paper are promising, however a more elaborate investigation into the underlying mechanisms have not been presented here. Additional characterization like X-ray diffraction, IR-spectroscopy, and X-ray photoelectron spectroscopy would have revealed valuable data, but within the scope if this project that was not feasible. The luminescence thermometry investigation presented in this work serves as a proof-of-concept, however more detailed characterization and data analysis would be required to develop a better understanding of the potential that the presented CDs have.

4 CONCLUSIONS

This thesis has demonstrated the synthesis and characterization of bio-based carbon dots (CDs) from xylose extracted from almond shells, focusing on their application in thermometry. By doping the CDs with *ortho*-phenylenediamine, we effectively tuned their photoluminescent properties, achieving emission in longer wavelength regions crucial for biological applications. The synthesized CDs displayed desirable fluorescent properties, and temperature-dependent luminescence, enabling single-band luminescence thermometry. However, challenges remain in understanding the underlying fluorescent mechanisms due to the observer variability. Further refinement is needed in future research to fully harness the potential of bio-based CDs in nanothermometry and related fields.

5 REFERENCES

1. Gan, J.; Chen, L.; Chen, Z.; Zhang, J.; Yu, W.; Huang, C.; Wu, Y.; Zhang, K. Lignocellulosic Biomass-Based Carbon Dots: Synthesis Processes, properties, and applications. *Small* **2023**, *19* (48).
2. Lim, S. Y.; Shen, W.; Gao, Z. Carbon quantum dots and their applications. *Chemical Society Reviews* **2015**, *44* (1), 362–381. https://doi.org/10.1039/c4cs00269e
3. Hola, K.; Zhang, Y.; Wang, Y.; Giannelis, E. P.; Zboril, R.; Rogach, A. L. Carbon dots—Emerging light emitters for bioimaging, cancer therapy and optoelectronics. *Nano Today* **2014**, *9* (5), 590–603. https://doi.org/10.1016/j.nantod.2014.09.004
4. Wang, C.; Lin, H.; Xu, Z.; Huang, Y.; Humphrey, M. G.; Zhang, C. Tunable Carbon-Dot-Based Dual-Emission fluorescent nanohybrids for ratiometric optical thermometry in living cells. *ACS Applied Materials & Interfaces* **2016**, *8* (10), 6621–6628. https://doi.org/10.1021/acsami.5b11317
5. Zhou, J.; Del Rosal, B.; Jaque, D.; Uchiyama, S.; Jin, D. Advances and challenges for fluorescence nanothermometry. *Nature Methods* **2020**, *17* (10), 967–980. https://www.nature.com/articles/s41592-020-0957-y
6. European Commission. *Critical raw materials*. Internal Market, Industry, Entrepreneurship and SMEs. https://single-market-economy.ec.europa.eu/sectors/raw-materials/areas-specific-interest/critical-raw-materials_en (accessed 2024-07-12)
7. La Ferla, B.; Vercelli, B. Red-Emitting Carbon Quantum Dots for Biomedical applications: Synthesis and purification issues of the Hydrothermal approach. *Nanomaterials* **2023**, *13* (10), 1635. https://doi.org/10.3390/nano13101635
8. Masha, S.; Oluwafemi, O. S. Cost-effective synthesis of red-emitting carbon-based quantum dots and its photothermal profiling. *Materials Letters* **2022**, *323*, 132590. https://doi.org/10.1016/j.matlet.2022.132590
9. Ju, Y. J.; Li, N.; Liu, S. G.; Liang, J. Y.; Gao, X.; Fan, Y. Z.; Luo, H. Q.; Li, N. B. Proton-controlled synthesis of red-emitting carbon dots and application for hematin detection in human erythrocytes. *Analytical and Bioanalytical Chemistry/Analytical & Bioanalytical Chemistry* **2019**, *411* (6), 1159–1167. https://doi.org/10.1007/s00216-018-1547-z
10. Rodríguez-Carballo, G.; García-Sancho, C.; Algarra, M.; Castro, E.; Moreno-Tost, R. One-Pot Synthesis of Green-Emitting Nitrogen-Doped Carbon Dots from Xylose. *Catalysts* **2023**, *13* (10), 1358. https://doi.org/10.3390/catal13101358
11. Wang, J.; Wang, J.; Xiao, W.; Geng, Z.; Tan, D.; Wei, L.; Li, J.; Xue, L.; Wang, X.; Zhu, J. Lignin-derived red-emitting carbon dots for colorimetric and sensitive fluorometric detection of water in organic solvents. *Analytical Methods* **2020**, 12 (25), 3218–3224. https://doi.org/10.1039/d0ay00485e
12. Zhu, Z.; Yang, P.; Chen, M.; Zhang, T.; Cao, Y.; Zhang, W.; Chen, W. Microwave synthesis of amphiphilic carbon dots from xylose and construction of luminescent composites with shape recovery performance. *Journal of Luminescence* **2019**, 213, 474–481. https://doi.org/10.1016/j.jlumin.2019.05.006
13. Yang, P.; Zhu, Z.; Chen, W.; Luo, M.; Zhang, W.; Zhang, T.; Chen, M.; Zhou, X. Nitrogen/sulfur Co-doping strategy to synthesis green-yellow emitting carbon dots derived from xylose: Toward application in pH sensing. *Journal of Luminescence* **2020**, 227, 117489. https://doi.org/10.1016/j.jlumin.2020.117489

14. Zhu, S.; Song, Y.; Zhao, X.; Shao, J.; Zhang, J.; Yang, B. The photoluminescence mechanism in carbon dots (graphene quantum dots, carbon nanodots, and polymer dots): current state and future perspective. *Nano Research* **2015**, *8* (2), 355–381. https://doi.org/10.1007/s12274-014-0644-3

15. Ding, H.; Yu, S.-B.; Wei, J.-S.; Xiong, H.-M. Full-Color Light-Emitting Carbon Dots with a Surface-State-Controlled Luminescence Mechanism. *ACS Nano* **2015**, *10* (1), 484–491. https://doi.org/10.1021/acsnano.5b05406

16. Manioudakis, J.; Victoria, F.; Thompson, C. A.; Brown, L.; Movsum, M.; Lucifero, R.; Naccache, R. Effects of nitrogen-doping on the photophysical properties of carbon dots. *Journal of Materials Chemistry. C* **2019**, *7* (4), 853–862. https://doi.org/10.1039/c8tc04821e

17. Miao, S.; Liang, K.; Zhu, J.; Yang, B.; Zhao, D.; Kong, B. Hetero-atom-doped carbon dots: Doping strategies, properties and applications. *Nano Today* **2020**, *33*, 100879. https://doi.org/10.1016/j.nantod.2020.100879

18. Wang, L.; Choi, W. M.; Chung, J. S.; Hur, S. H. Multicolor Emitting N-Doped Carbon Dots Derived from Ascorbic Acid and Phenylenediamine Precursors. *Nanoscale Research Letters* **2020**, *15* (1). https://doi.org/10.1186/s11671-020-03453-3

19. Wang, B.; Lu, S. The light of carbon dots: From mechanism to applications. *Matter* **2022**, *5* (1), 110–149. https://doi.org/10.1016/j.matt.2021.10.016

20. Queirós, C. S. G. P.; Cardoso, S.; Lourenço, A.; Ferreira, J.; Miranda, I.; Lourenço, M. J. V.; Pereira, H. Characterization of walnut, almond, and pine nut shells regarding chemical composition and extract composition. *Biomass Conversion and Biorefinery* **2019**, *10* (1), 175–188. https://doi.org/10.1007/s13399-019-00424-2

21. Wang, Z.; Fu, B.; Zou, S.; Duan, B.; Chang, C.; Yang, B.; Zhou, X.; Zhang, L. Facile construction of carbon dots via acid catalytic hydrothermal method and their application for target imaging of cancer cells. *Nano Research* **2016**, *9* (1), 214–223. https://doi.org/10.1007/s12274-016-0992-2

22. Dramićanin, M. D. Trends in luminescence thermometry. *Journal of Applied Physics* **2020**, *128* (4). https://doi.org/10.1063/5.0014825

23. Bednarkiewicz, A.; Marciniak, L. D.; Carlos, D.; Jaque, D. Standardizing luminescence nanothermometry for biomedical applications. *Nanoscale* **2020**, *12*, 14405–14421. https://doi.org/10.1039/d0nr03568h

6 SUPPORTING INFORMATION

6.1 CHEMICAL AND MATERIALS

- 1,2-Phenylenediamine (Tokyo Chemical Industry Ltd.)
- Universal Indicator Paper, pH 1-11 (Johnson® TEST PAPERS, 004.5)
- 0.2 µL syringe filter, 25mm (CHROMAFIL®Xtra PVDF-20/25)
- Dialysis tubing (1 kD), Spectra/Por®7 Dialysis Membrane
- Deionized and (type I) Milli-Q water
- Teflon lined stainless steel autoclave (50mL)
- Xylose extracted from almond shells (see section 6.3)
- Ammonia, NH_3 in H_2O solution (Honeywell, 30-33 WT %)
- Carbon on copper TEM grids
- Carbon Tape
- Quartz cuvette

6.2 EQUIPMENT

- Muffle furnace, *Carbolite* CWF 11/5
- Transmission Electron Microscope, *JEOL* JEM-F200
- Scanning Electron Microscope, *FEI* Quanta 600 FEG ESEM
- Fluorescence spectrometer, *Zolix* OmniFluo900, with a PMT detector and continuum Xenon light source (owned and operated by *Institute of Chemical Research of Catalonia, ICIQ*)
- Fluorescence spectrometer, *Horiba Jobin Yvon* Fluorolog, equipped with Peltier heater module, a photomultiplier, double monochromator, and Xenon light source (owned and operated by *Institute of Chemical Research of Catalonia, ICIQ*)

6.3 XYLOSE EXTRACTION

The xylose extraction procedure was developed and executed in a routine way in the research group. 5 grams of ground almond shells and 50 ml of a H_2SO_4 solution (1% aq.) was added to a microwave compatible autoclave. The reaction time was 1 hour and 40 minutes under microwave radiation. The product was vacuum filtered, and the resulting filtrate was dried to solidify the extract. This extract contains xylose and some other biomolecules.

6.4 ADDITIONAL RESULTS

6.4.1 Photoluminescence

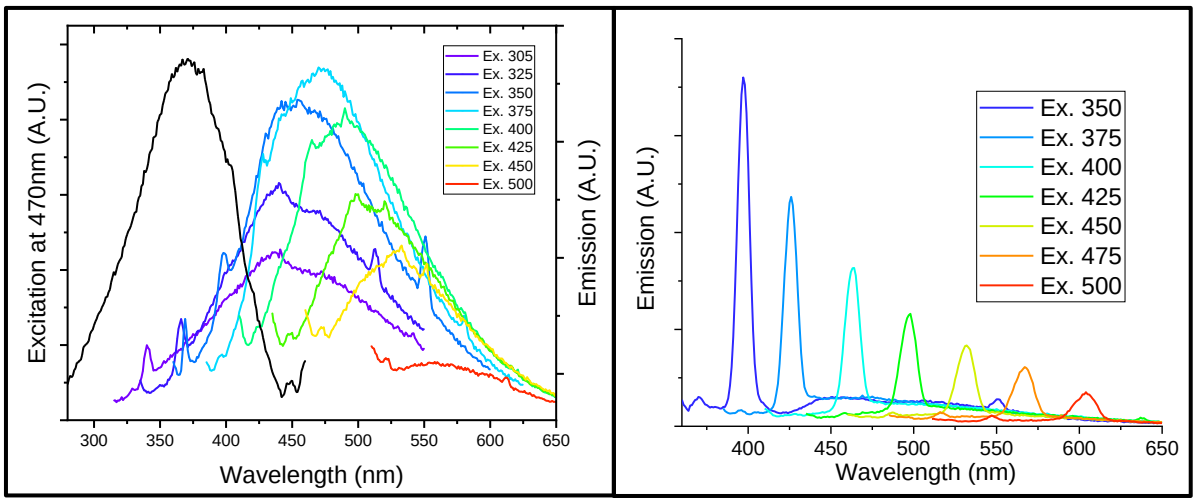

Figure 9: Left: Emission spectrum at different excitation wavelengths for CD-12h that was freeze-dried and stored in a conventional fridge for more than a week. The solids (1.3 mg) were dispersed in deionized water (5 ml) for the measurement. Right: Emission spectrum at different excitation wavelengths for deionized water.